 ©2006 Kvantovaya Elektronika and Turpion Ltd

PACS numbers: 87.50.Kk; 43.35.Sx
DOI: 10.1070/QE2006v036n12ABEH013262

Opto-acoustic diagnostics of the thermal action of high-intensity focused ultrasound on biological tissues: the possibility of its applications and model experiments

T.D. Khokhlova, I.M. Pelivanov, O.A. Sapozhnikov, V.S. Solomatin, A.A. Karabutov

***Abstract*. The possibility of using the opto-acoustic (OA) method for monitoring high-intensity ultrasonic therapy is studied. The optical properties of raw and boiled liver samples used as the undamaged model tissue and tissue destroyed by ultrasound, respectively, are measured. Experiments are performed with samples consisting of several alternating layers of raw and boiled liver of different thickness. The position and transverse size of the thermal lesion were determined from the temporal shape of the OA signals. The results of measurements are compared with the real size and position of the thermal lesion determined from the subsequent cuts of the sample. It is shown that the OA method permits the diagnostics of variations in biological tissues upon ultrasonic therapy.**

Keywords: *opto-acoustic diagnostic method, biological tissues, high-intensity ultrasound.*

1. Introduction

High-intensity focused ultrasound (HIFU) finds increasing applications in various fields of medicine. The basic scheme of the HIFU application is shown in Fig. 1. A focused ultrasonic transducer is placed near the human body surface. The ultrasonic intensity near the transducer surface is too low to heat tissues and cause their damage; however, in the focal area the ultrasonic intensity is increased dramatically and tissue is heated due to the absorption of acoustic waves. In a certain period of time, the ultrasonic heating can result in the thermal damage of proteins. This effect is used for the 'occlusion' of blood vessels in treating internal haemorrhages, in the therapy of tumours, and a number of other medical applications [1 – 3]. HIFU therapy causes the coagulative necrosis of a tumour, which then is 'dissolved' by organism. In addition, it was found that this treatment causes the enhanced immune response [2] preventing the recurrent growth of the tumour. As a rule, a lesion produced by ultrasound has the shape of a cigar [4] of length 0.5 – 1 cm and transverse size of 2 – 3 mm. To damage a large mass of tissue, the focus of a transducer is scanned over the required region [5, 6].

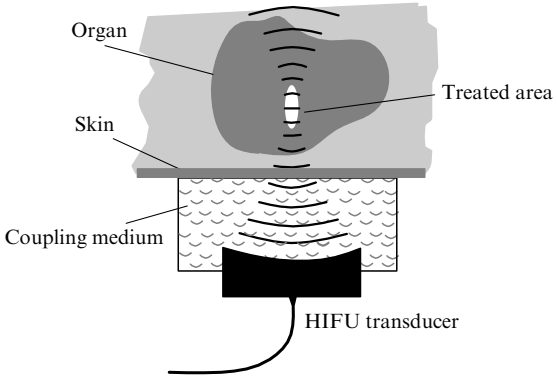

Figure 1. Diagram of the high-intensity focused ultrasound treatment.

Thus, HIFU can be used for the noninvasive tumour surgery. However, the main factor preventing clinical HIFU applications is the inadequate development of the methods for targeting and therapy monitoring. At present, MRI and various ultrasonic methods are used for this purpose.

The use of NMR tomography to control HIFU therapy is based on the temperature dependence of the shift of the Larmor frequency of water (and, correspondingly, the phase of the MR signal) [6]. Since certain thermal dose is required to cause the coagulative necrosis of tissue, the real-time emperature monitoring allows one to estimate the size and shape of the lesion. This method is now rather widely used and is already used in clinics [7, 8]. A substantial disadvantage of the method is that the distribution of the critical thermal dose not always corresponds to the region of coagulative necrosis of tissue. For example, if the treated region contains a large blood vessel, the heat is drained by perfusion that can prevent the tissue damage. In addition, a patient moves during measurements (breathing, heartbeat), which leads to considerable artefacts in the temperature distributions obtained.

The heating and thermal coagulation of a tissue is accompanied by a change in its acoustic properties such as the shear modulus, absorption coefficient, and ultrasound velocity in it. This is used in a number of methods for controlling the HIFU therapy [9 – 11]. In these methods, the distortion of the ultrasonic probe pulse shape or the change

T.D. Khokhlova, I.M. Pelivanov, V.S. Solomatin, A.A. Karabutov
International Laser Center, M.V. Lomonosov Moscow State University, Vorob'evy gory, 119992 Moscow, Russia;
e-mail: t_khokhlova@ilc.edu.ru, pelivanov@ilc.edu.ru;
O.A. Sapozhnikov Department of Physics, M.V. Lomonosov Moscow State University, Vorob'evy gory, 119992 Moscow, Russia;
e-mail: oleg@acs366.phys.msu.ru

Received 29 May 2006; revision received 5 July 2006
Kvantovaya Elektronika **36** (12) 1097 – 1102 (2006)
Translated by M.N. Sapozhnikov

in its arrival time caused by the influence of focused ultrasound on tissue is measured with ultrasonic pulse-echo scanners. Ultrasonic methods yield good results under laboratory conditions and allow the visualisation of the thermal lesion of the tissue. However, *in vivo* applications of these methods involve a number of technical difficulties, and they are not employed in clinics so far.

Note also that during HIFU therapy, bubbles appear in the focal region, which are clearly observed on the screen of a standard diagnostic ultrasonic system due to strong scattering of ultrasound by them [12]. This effect can be used for aiming to the required region; however, it cannot be employed for the visualisation of the thermal lesion.

In this paper, we propose a new opto-acoustic (OA) method for visualisation of the thermal lesion during ultrasonic therapy. The method is based on the thermooptic effect [13] when the absorption of pulsed laser radiation in a medium is accompanied by the heating and pulsed expansion of the medium, resulting in the generation of broadband ultrasonic signals, which are called OA signals. The temporal profile of such signals is determined by the distribution of the heat release in the medium, thereby containing information on the absorption of light in it. Therefore, the distribution of absorbing optical inhomogeneities in the medium can be determined from the temporal profile of the recorded OA signal.

It was shown in a number of papers that the OA method can be used for the early breast cancer diagnostics [14]. The method is based on the fact that a cancerous tumour rapidly grows and, therefore, contains a higher amount of blood, which is the main chromophore in the near-IR region. Upon laser irradiation, the tumour becomes a source of OA signals. The temporal profile of these signals characterises the tumour shape and position. Similarly, if the optical properties of the thermal lesion differ from those of the undamaged tissue, they can be visualised by the OA method.

The aim of this paper was to demonstrate the principal possibility of using the OA method for the visualisation of HIFU damages of biological tissues.

2. Materials and methods

To study the applicability of the OA method for monitoring the HIFU therapy, it is necessary first of all to measure the absorption μ_a and effective attenuation $\mu_{eff} = (3\mu_a\mu_s')^{1/2}$ coefficients of a biological tissue [15] [where $\mu_s' = \mu_s(1-g)$ in the reduced scattering coefficient and g is the scattering anisotropy factor] before and after coagulation caused by ultrasonic heating. As a biological tissue we used a porcine liver. Samples of width 3–4 cm and thickness $\sim$2 cm cut from the porcine liver were placed into distilled water and were kept for some time in a vessel at a reduced pressure of about 0.5 atm. The aim of this procedure was to remove gas bubbles from the tissue (degassing). Gas bubbles lead to attenuation of ultrasound distorting the temporal profile of the OA signal excited in the tissue.

Samples of a coagulated tissue were prepared by placing the degassed samples of fresh liver into water at a temperature close to 100 °C, where they were kept for about 10 min and then again degassed.

The OA study of samples was performed before and after their temperature treatment. OA signals were excited by a 1064-nm pulsed Nd : YAG laser. A wide laser beam (3 cm in diameter) was incident onto a sample surface and the resulting OA signal was detected with a piezoelectric transducer made of a polyvinyldenfluoride film glued on a flat damping surface. The transducer had the form of a disc of thickness 110 μm and diameter 8 mm. This provided an almost uniform sensitivity in the frequency range from 0.05 to 2 MHz equal to 845 μV Pa^{-1} after fifty-fold amplification. The effective attenuation coefficient was measured by exciting and detecting OA signals at the opposite sides of a sample (forward mode), while the absorption coefficient was measured by exciting and detecting AO signals at the same side of a sample (backward mode). The diagram of the setup and the measurement method are described in detail in [15].

In order to investigate how the lesion located inside the intact biological tissue influences the shape of excited OA signal, we used special phantom media. These media consisted of alternating layers of boiled and raw porcine liver with known thickness pressed against each other and placed in degassed water. The OA study of such samples was performed in the forward mode by employing the same setup as for measuring the effective attenuation coefficient.

In the final experiment we used a porcine liver sample in which the thermal lesion was produced by HIFU. In this case, the coagulated region was produced inside the sample and was invisible from the surface, i.e. its exact position and size were unknown beforehand. Figure 2 shows the diagram of the experimental setup for producing an lesion inside tissues. The signal from athe function generator was amplified and fed to a spherically focusing PZT ceramics transducer operating at the frequency of 1.092 MH. The diameter of the transducer was 10 cm and the focal length was also 10 cm. The transducer was fixed in a bath with distilled degassed water. Pig liver samples were fixed in a special holder so that the focus of the ultrasonic beam was at the sample centre. The samples were exposed to ultrasonic radiation for 20 s. The acoustic intensity at the transducer focus measured in water with a needle hydrophone was 1208 W cm^{-2}. Taking into account the decay of ultrasound in liver (0.3 dB cm^{-1} at a frequency of 1.1 MHz [16]), this intensity was $\sim$1000 W cm^{-2}. Because liver samples were

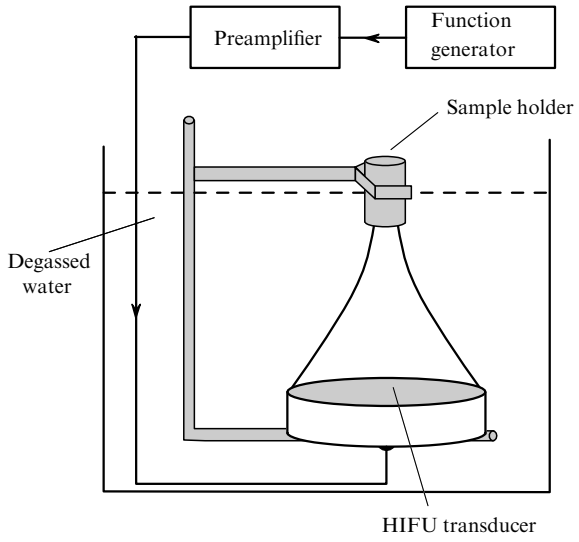

Figure 2. Diagram of the experimental setup for producing thermal lesion in porcine liver samples.

completely immersed in water, the ultrasonic beam propagated through the liver came out again to water, which excluded the reflection of sound waves from the upper surface of the sample and the formation of standing waves. Note also that liver samples were degassed before ultrasonic irradiation to avoid the cavitation of bubbles present in the liver in a strong ultrasonic field.

Let us estimate the temperature change in tliver at the focus of the ultrasonic transducer in order to compare it with the heating regime during the preparation of boiled samples. If the heat conduction is neglected, a change in the temperature caused by the absorption of ultrasound in a linear regime is described by the expression

$$\frac{\mathrm{d}T}{\mathrm{d}t} = \frac{2\alpha}{\rho c_p} I, \tag{1}$$

where T is the temperature; I is the acoustic intensity at the transducer focus; α is the absorption coefficient of ultrasound in tissue; ρ is the tissue density; and c_p is the tissue specific heat. By substituting the corresponding parameters for porcine liver [16] into (1), we see that the temperature 100 °C is achieved already after 4.5 s. The heat conduction mechanism will, of course, slow down somewhat the tissue heating. However, the characteristic heat transfer time, which can be estimated as

$$t = \frac{\rho c_p a^2}{\chi} \tag{2}$$

(where a is the ultrasonic beam waist radius and χ is the heat conductivity) is 14 s in our case. Thus, the boiling point is achieved earlier than the heat conduction becomes a concern. Therefore, the liver boiled at the temperature 100 °C can be considered as an adequate model of HIFU lesion.

The OA diagnostics of the lesion region was performed by using the same setup as for measuring the effective attenuation coefficient (forward mode). However, instead of a broad laser beam, the beam of diameter about 2 mm was used, which was scanned across the sample (Fig. 3a). This allowed us to localise the lesion, which, as mentioned above, was not noticeable from the sample surface. After OA measurements, the sample was cut to determine accurately the size and position of the lesion and compare them with the data obtained from analysis of the temporal shape of OA signals. The typical section of a sample is shown in Fig. 3b.

3. Experimental results

3.1 Measurement of optical properties

The aim of the first series of experiments was the measurement of the light effective attenuation μ_{eff} and absorption μ_{a} coefficients in raw and boiled liver at the wavelength of 1064 nm. We studied eight samples. The effective attenuation coefficient was measured in the forward mode of OA signal detection. Figure 4 shows the OA signals obtained from raw and boiled liver samples. One can see that the leading edge of signals can be well approximated by an exponential [curves (*2*)] with the exponent equal to the effective attenuation coefficient [17]. The leading edge of the OA signal from the boiled liver sample is considerably steeper that that from the raw liver

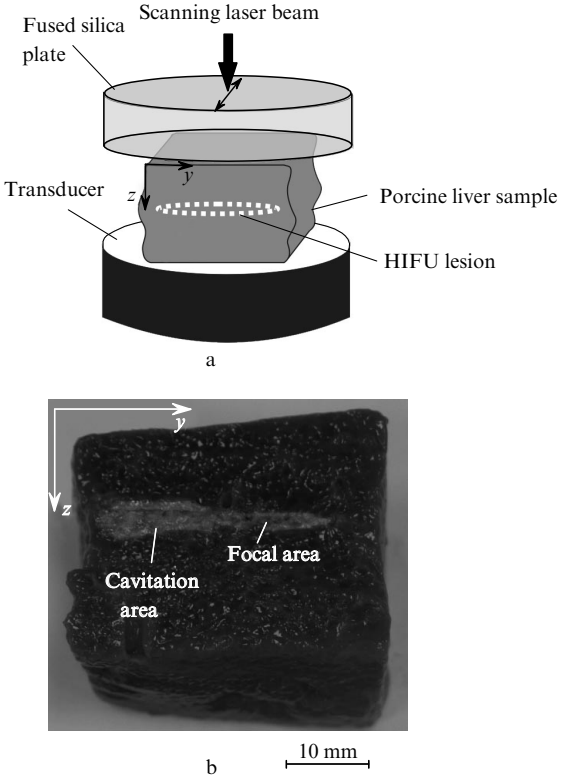

Figure 3. Diagram of the OA diagnostics of porcine liver sample containing a thermal lesion (a) and the sample cross section (b).

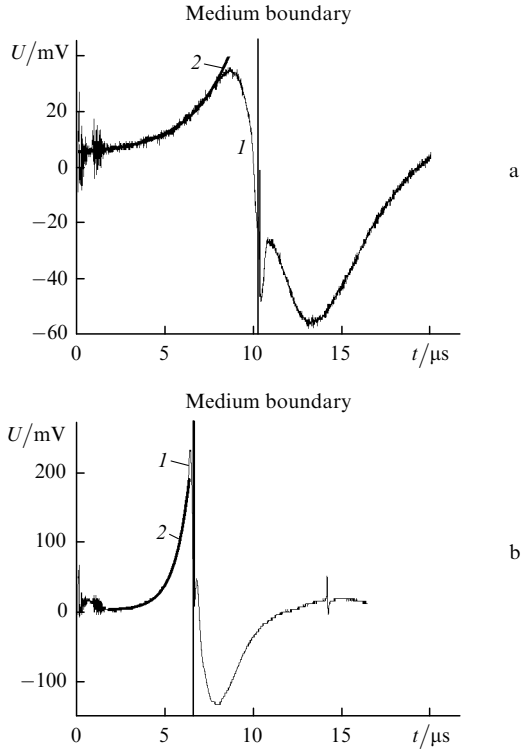

Figure 4. Opto-acoustic signals (*1*) from raw (a) and boiled (b) liver samples obtained in the forward mode and the exponential approximation of the leading edge of signals (*2*).

sample, which suggests that the effective attenuation coefficient of the boiled liver sample is higher.

The absorption coefficient μ_a was measured in the backward mode when OA signals were excited and detected at the same side of the sample. The measurement principle is based on the fact that the OA signal intensity (the peak acoustic pressure p) is proportional to the absorption coefficient, $p \sim \mu_a$. Therefore, by measuring the OA signal p^{ref} from a reference medium with the known absorption coefficient μ_a^{ref}, we can calculate the absorption coefficient of the medium under study:

$$\mu_a = \frac{p}{p^{ref}} \mu_a^{ref}. \quad (3)$$

We used milk as a reference medium, in which the absorption coefficient is $0.18\ cm^{-1}$ at 1064 nm [17]. Knowing the absorption and effective attenuation coefficients, we can calculate the reduced scattering coefficient [15]:

$$\mu_s' = \frac{\mu_{eff}^2}{3\mu_a}.$$

Figure 5 presents OA signals from raw and boiled liver samples and the reference medium (milk) detected in the backward mode. Optical properties calculated from the results of measurements are presented in Table 1. There is some variation in the obtained values of μ_{eff}, μ_a, and μ_a' from sample to sample. However, in all the samples the absorption and scattering coefficients for the boiled liver were always approximately twice higher than these for the raw liver.

3.2 Diagnostics of optical absorption in a layered tissue

Figure 6a shows the OA signal from a sample consisting of a raw liver layer of thickness about 8 mm and a boiled liver layer of thickness about 7 mm. The peak at 4 μs corresponds to the near-surface laser radiation intensity maximum at the upper boundary of the medium. The exponential front following the peak corresponds to the decay profile of light in the raw liver layer. The peak at 4 μs corresponds to the arrival of a signal from the raw–boiled liver layer interface. The rise of this peak is determined by the fact that the absorption in boiled liver is higher than that in raw liver and, hence, there is a step in the heat release distribution at the interface. The zero time delay corresponds to the signal from the sample surface pressed against the transducer. The thicknesses of layers can be determined quite accurately from the time delay between the arrival of signals from the sample surface and interface between the two media. The numbers in parentheses in Fig. 6 are the thickness of layers calculated by the duration of the corresponding parts of the signal taking into account the sound speed in liver (1550 m s^{-1} [16]). One can see that these thicknesses are close to their true values.

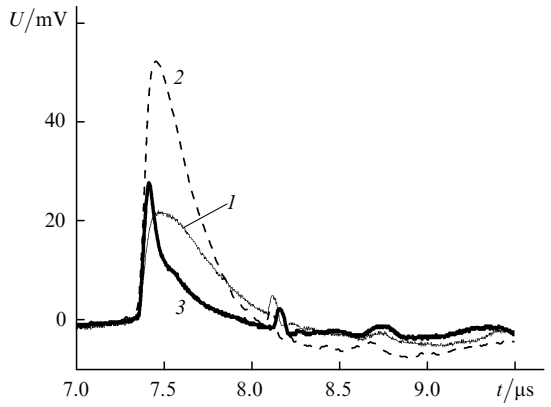

Figure 5. Opto-acoustic signals from raw (*1*) and boiled (*2*) liver samples and milk (*3*) obtained in the backward mode.

Table 1. Optical parameters of boiled and raw porcine liver ($\lambda = 1064$ nm).

Sample	μ_a/cm^{-1}	μ_{eff}/cm^{-1}	μ_s/cm^{-1}
Raw porcine liver	0.17 ± 0.05	2.8 ± 0.2	15 ± 5

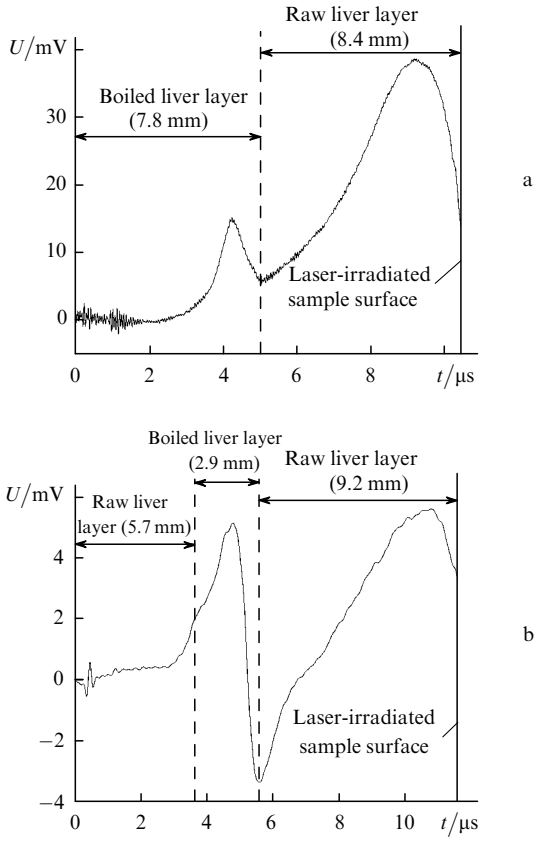

Figure 6. Opto-acoustic signals obtained in the forward mode from samples consisting of two (a) and three (b) alternating layers of raw and boliled liver.

Because a single damage caused by high-intensity ultrasound has an elongated shape and its transverse size is 2–3 mm, it is interesting to obtain the OA signal from a thin (~3 mm) layer of boiled liver located between two rather thick (~10 mm) layers of raw liver. This signal is shown in Fig. 6b. The 12-μs time delay corresponds to the time of signal arrival from the upper boundary of the sample. The near-surface maximum is followed by a rather smooth exponential front repeating the decay profile of light in the tissue. The local maximum at 5 μs, as in Fig. 6a, is related to a jump in the absorption coefficient at the raw–boiled liver layer interface. The local minimum at 6 μs is most likely related to the presence of an air bubble or water

between the layers. The arrival time of the OA signal from the interface between the lower layer of raw liver and the intermediate layer of boiled liver is about 3.5 μs. At this moment the temporal profile of the signal bends, and its exponential front becomes less steep, which suggests that the effective attenuation coefficient in the lower layer decreases compared to that in the intermediate layer. Thus, the temporal profile of the OA signal has specific features (the local maximum and bend), which make it possible to determine the positions of the upper and lower boundaries of a flat thin coagulated layer and, therefore, its thickness.

3.3 Diagnostics of the HIFU lesion

To localise the lesion, a narrow laser beam was scanned across a sample surface (see Fig. 3a) and the excited OA signals were detected in the forward mode. The OA signal obtained when the laser spot was located directly over the assumed lesion of the tissue is shown in Fig. 7a. The smooth leading edge of the signal, corresponding to light attenuation in raw liver, contains a short burst that indicates an object with a higher absorption coefficient located within the tissue. The duration of this burst gives the estimate of the transverse size (1.8 mm) of the coagulated tissue region and of its position with respect to sample surface.

The signal shown in Fig. 7b was obtained when the laser spot was located near the sample edge, so that even the laser beam broadened due to scattering did not reach the coagulated region. One can see that the signal front is smooth and does not contain any features, which suggests that the medium is homogeneous over depth in this position of the laser beam.

After OA experiments, the sample was cut along the lesion (see Fig. 3b). One can see that, except a classical cigar-like lesion produced directly near the focus of the ultrasonic beam, there is a broader lesion of an irregular shape, which is displaced from the focus towards the transducer. This region appears due to the cavitation of bubbles remained in the tissue. The transverse size of the thermal lesion, which was tentatively irradiated by the laser beam during OA measurements, is about 2 mm, in accordance with the value obtained from the OA signal shape.

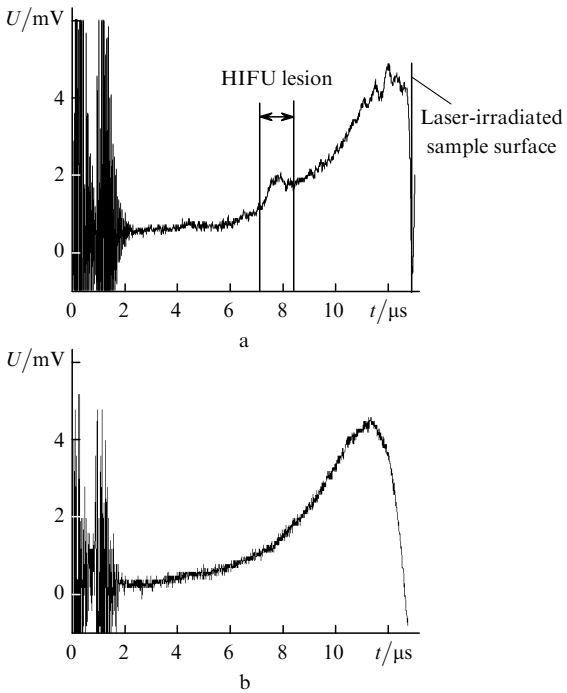

Figure 7. Opto-acoustic signals from a porcine liver sample containing a therma lesion obtained when the laser spot was located over the assumed lesion location (a) and near the sample edge (b).

4. Discussion

Let us now analyse the most interesting results obtained in the paper.

As follows from Table 1, the absorption coefficient in the coagulated liver is at least twice as large as that in the undamaged liver. This can be explained by structural changes produced in haemoglobin upon its heating resulting in the formation of methaemoglobin in which absorption at 1064 nm is several times higher than in haemoglobin [18]. Note here that, although during the preparation of samples a considerable amount of blood came out to water, samples were pink during measurements, indicating to the presence of blood in microcapillaries. It seems that during *in vivo* measurements, i.e. at high concentrations of blood, the increase in the absorption coefficient of the coagulated tissue will be manifested stronger.

An increase in the reduced scattering coefficient can be caused by several factors. First, it was shown in [19] that the average effective size of scattering centres (in terms of the Mie theory) decreases after the tissue coagulation, which results in a decrease in the scattering anisotropy factor g, i.e. scattering becomes more isotropic. This can be explained [19] by the formation of new structural components of the tissue due to coagulation and appearance of vacuoles in cytoplasm caused by heating. Second, coagulation causes the tissue dehydration, thereby reducing its volume, while the amount of absorbing and scattering centres remains invariable, i.e. their concentration in the unit volume increases [20, 21]. As a result, both the scattering coefficient μ_s and absorption coefficient μ_a can increase.

We have shown that a drastic increase in absorption occurs at the boundary of the lesion, which can be detected by the OA method.

We have considered in this paper the lesion of a rather large size (25 × 3 mm) located at a relatively small depth (1 cm). The OA signals were detected using the forward mode requiring the two-side access to a sample, which restricts its applications in many practical cases. In addition, the one-element detection scheme does not allow the imaging of an absorbing object; therefore, it would be convenient to use a multielement array of detectors for monitoring HIFU therapy. For example, the 32-element antenna described in [22] allows the imaging of absorbing objects with a spatial resolution of 2 mm.

The maximum depth at which the lesion can be detected depends strongly on the penetration depth of light to the tissue under study. For example, it was shown in [23] that an object of size 3 mm in a human breast, in which absorption is twice as large as that in the environment, can be detected by the OA method at a depth of up to 3.5 cm. On the contrary, the penetration depth of light in organs containing a great amount of blood (liver, kidney) will be most likely small because blood strongly absorbs in the near-IR region

[24]. Therefore, the most probable application of the OA method for visualisation of lesions is the monitoring of the high-intensity ultrasonic therapy of the breast or prostate cancer. Another possible application of the OA method in high-intensity ultrasonic therapy is the control of the tissue temperature during ultrasonic irradiation. The matter is that the coefficient of thermal expansion of water, which determines the OA excitation efficiency, strongly increases with increasing temperature [16]. We plan to study the influence of this effect on the temporal shape of OA signals excited in tissues in the future.

5. Conclusions

We have shown in this paper the principal possibility of detecting the thermal lesion in biological tissues produced by focused ultrasound. The absorption and scattering coefficients have been measured at a wavelength of 1064 nm for raw and boiled liver samples, which simulated the intact and treated tissues, respectively. It has been shown that the scattering coefficient virtually does not change after thermal coagulation, whereas the absorption coefficient increases more than twice. In the forward mode of detection of ultrasonic pulses, the OA signals have been obtained from a sample in which a flat thin layer of boiled liver was located between the two layers of raw liver (model of the lesion located inside a tissue). The position of the boiled liver layer and its thickness could be determined from the temporal shape of the OA signal. The thermal damage of the tissue inside the porcine liver sample was produced by focused ultrasound and the sample was studied then by the OA method. The OA signal from the region damaged by ultrasound was distinctly observed on the front of the signal from the undamaged tissue. The position and transverse size of the damage determined from the temporal shape of the signal were in agreement with their real values. The results obtained in this study demonstrate the possibility of using the OA method for visualisation of thermal lesion induced by HIFU.

References

1. Siegal R.J., Vaezy S., Martin R., Crum L. *Echocardiography: A J. of CV Ultrasound & Allied Tech*., **18**, 309 (2001).
2. Wu F., Wang Z.-B., Lu P., Xu Z.-L., Chen W.-Z., Zhu H., Jin C.-B. *Ultrasound Med. Biol*., **30**, 1217 (2004).
3. Baily M.P., Khokhlova V.A., Sapozhnikov O.A., Cargl S.G., Cram L.A. *Acoust. Zh*., **49**, 437 (2003).
4. Hill C.R., Bamber J.C., ter Haar G.R. *Physical Principles of Medical Ultrasonics* (England, Chichester, John Wiley & Sons Ltd., 2002).
5. Malcolm A.R., ter Haar G.R. *Ultrasound Med. Biol*., **22**, 659 (1996).
6. Diederich C.J., Hynynen K. *Ultrasound Med. Biol*., **25**, 871 (1999).
7. Ishikara Y., Calderon A., Watanabe H., Okamoto K., Suzuki Y., Kuroda K., Suzuki Y. *Magn. Reson. Med*., **34**, 814 (1995).
8. Hynynen K., McDannold N. *Int. J. Hyperthermia*, **20**, 725 (2004).
9. Baker L.A.S., Bamber J.C. *Proc. British Medical Ultrasound Society 34th Annual Scientific Meeting* (Manchester, 2002) p. 3.
10. Miller N.R., Bamber J.C., ter Haar G.R. *Ultrasound Med. Biol*., **30**, 345 (2003).
11. Ophir J., Alam S.K., Garra B.S., Kallel F., Konofagou E., Krouskop T.A., Merritt C.R.B., Righetti R., Souchon R., Srinivasan S., Varghese T. *J. Med. Ultrasonics*, **29**, 155 (2003).
12. Vaezy S., Shi X., Martin R.W., Chi E., Nelson P.I., Bailey M.R., Crum L.A. *Ultrasound Med. Biol*., **27**, 33 (2001).
13. Gusev V.E., Karabutov A.A. *Lazernaya optoakustika* (Laser Optoacoustics) (Moscow: Nauka, 1991).
14. Andreev V.G., Karabutov A.A., Solomatin S.V., Savateeva E.V., Aleynikov V.L., Zhulina Y.V., Fleming R.D., Oraevsky A.A. *Proc. SPIE Int. Soc. Opt. Eng*., **3916**, 36 (2000).
15. Pelivanov I.M., Belov S.A., Solomatin V.S., Khokhlova T.D., Karabutov A.A. *Kvantovaya Elektron*., **36**, 1089 (2006) [*Quantum Electron*., **36**, 1089 (2006)].
16. Duck F.A. *Physical Properties of Tissue. A Comprehensive Reference Book* (London, San Diego, New York, Boston: Acad. Press, 1990).
17. Grashin P.S., Karabutov A.A., Oraevsky A.A., Pelivanov I.M., Podymova N.B., Savatevea E.B., Solomatin V.S. *Kvantovaya Elektron*., **32**, 868 (2002) [*Quantum Electron*., **32**, 868 (2002)].
18. Black J.F., Barton J.K. *Photochem. Photobiol*., **80**, 89 (2004).
19. Nilsson A.M.K., Sturesson C., Liu L.D., Andersson-Engels S. *Appl. Opt*., **37**, 1256 (1998).
20. Cilesiz I.F., Welch A.J. *Appl. Opt*., **32**, 477 (1993).
21. Yaroslavsky A.N., Schulze P.C., Yaroslavsky I.V., Schober R., Ulrich F., Schwarzmaier H.-J. *Phys. Med. Biol*., **47**, 2059 (2002).
22. Kozhushko V., Khokhlova T., Zharinov A., Pelivanov I., Solomatin V., Karabutov A. *J. Acoust. Soc. Am*., **116**, 1498 (2004).
23. Khokhlova T.D., Pelivanov I.M., Kozhushko V.V., Zharinov A.N., Solomatin V.S., Karabutov A.A. *Appl. Opt*. (in press).
24. Taroni P., Pifferi A., Torricelli A., Comelli D., Cubeddu R. *Photochem. Photobiol. Sci*., **2**, 124 (2003).